

Diamond at 800 GPa

D. K. Bradley, J. H. Eggert, R. F. Smith, S. T. Prisbrey, D. G. Hicks, D. G. Braun, J. Biener,
A. V. Hamza, R. E. Rudd, and G. W. Collins

Lawrence Livermore National Laboratory, P.O. Box 808, Livermore, California 94551, USA

(Received 6 January 2008; published 18 February 2009)

A new compression technique, which enables the study of solids into the TPa regime, is described and used to ramp (or quasi-isentropically) compress diamond to a peak pressure of 1400 GPa. Diamond stress versus density data are reported to 800 GPa and suggest that the diamond phase is stable and has significant material strength up to at least this stress level. Data presented here are the highest ramp compression pressures by more than a factor of 5 and the highest-pressure *solid* equation-of-state data ever reported.

DOI: 10.1103/PhysRevLett.102.075503

PACS numbers: 62.50.-p, 52.50.Lp, 64.30.-t

The cores of Jupiter, Saturn, and many extra-solar planets likely contain material in the solid state at pressures (P) greater than 1 TPa (10 Mbar) [1]. What is the nature of a solid at such extreme pressures? On Earth, high- P solids are typically produced and studied using quasistatic diamond-anvil-cell (DAC) techniques, which have a natural high- P limit of ~ 300 GPa due to the mechanical strength of diamond [2,3]. Shock compression can produce significantly higher P than static experiments; however, shocks produce a significant temperature (T) increase so that above a few hundred GPa only properties of the fluid phase are typically explored. Thus, solid-state theories significantly above this range are untested. Ramp-wave compression (RWC) techniques (sometimes called quasi-isentropic compression) such as the one described here will extend the accessible pressure range for solid-state physics into the TPa regime.

The RWC technique is applied to diamond because of its importance in science and technology [4]. Diamond has been extensively studied, with static experiments mapping pressure density ($P - \rho$) to 140 GPa and high- P shocks exploring carbon through the diamond-melt transition [5–7]. However, many questions remain regarding the high- P solid phase, which until now was inaccessible. Using a temporally shaped radiation source [8], diamond was ramp-compressed to a peak pressure of 1400 GPa and the stress density ($P_x - \rho$) determined to 800 GPa. These data show that the diamond phase of carbon is stable and strong up to at least 800 GPa. Data presented here are the highest- P solid-state data ever collected and the highest- P ramp-wave data to date by more than a factor of 5 [9–11].

The diamond samples were 2 mm square freestanding plates, flat on one side and with four steps on the opposite side, $\sim 15/30/45/60$ μm thick, with each step 200 μm wide. The diamond samples were formed by chemical vapor deposition at 1050 K [4]. Interferometry was used to determine that the surface roughness was < 0.1 μm , thickness gradients were $< 1\%$, and step heights were accurate to 0.1 μm . Sample cross sections show a tightly

packed columnar crystal structure in the stress-loading direction with the grain size increasing from nanometer size at the nucleation sites on the stepped side to grain sizes approximately 30% of the step thickness on the drive side. X-ray diffraction showed a slight $\langle 111 \rangle$ texture in the growth direction. Samples were measured to be fully dense (3.51 g/cc) to within an accuracy of 0.1%. Each stepped sample was glued over a ~ 950 μm hole at one end of a gold hohlraum (Fig. 1) [8].

The inner walls of the hohlraum were illuminated with up to 21 beams of the Omega laser [12] with a combined energy up to 5700 J in a 3.5 ns temporally ramped pulse. This generated a spatially uniform distribution of thermal x rays with a characteristic radiation temperature T_r , which monotonically increased in time to a peak $T_r \sim 145$ eV [13]. The laser power, T_r , and resultant drive pressure

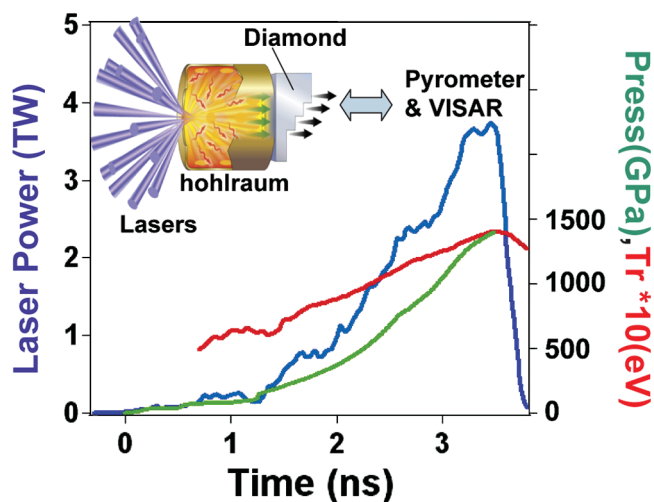


FIG. 1 (color). The inset shows a sketch of the target. Hohlräume had a diameter of 2 mm, a length of 2.24 mm, and a laser entrance hole diameter of 1.8 mm. The main figure shows incident laser intensity, characteristic temperature of the x-ray drive, and drive pressure on the diamond determined from the Lagrangian analysis.

versus time are shown in Fig. 1. The x-ray ablation of diamond produced a uniform ramped compression wave, which outran the thermal wave produced by ablation. As the compression wave reached the back surface of the diamond, the surface accelerated into free space, and the free-surface velocity history u_{fs} for each step was recorded with a line-imaging velocity interferometer (VISAR) [14]. A typical VISAR data record [Fig. 2(a)] had a spatial resolution of $\sim 5 \mu\text{m}$ over $\sim 800 \mu\text{m}$ at the target, a temporal resolution 0.01 ns over an 8 ns window, and minimum velocity per fringe of 3.3 km/s with the fringe position determined to less than 2% of a fringe. The space- and time-resolved thermal emission from the stepped diamond target was simultaneously recorded using a streaked optical pyrometer [Fig. 2(b)] [15].

For RWC to be near isentropic, the sample cannot be heated by external sources. Radiation hydrodynamic simulations, which give a good match to T_r , u_{fs} , and thermal emission, show that preheating of the bulk sample from high-energy x rays was insignificant compared to the plastic-work heating, and thermal conduction was too slow to affect these results. The free-surface temperature was estimated from the measured sample spectral radiance combined with the emissivity estimated from the measured VISAR reflectivity [16–18]. Figure 2(b) shows increases in spectral radiance at 4.0 and 4.5 ns which correlate with measured shock breakout in the 45 and 60 μm steps, respectively. The 15 μm step shows an initial rise at 3.3 ns, which correlates with the simulated increase in free-surface temperature. However, there is no detectable temperature rise for the unshocked 30 μm step. Using the analysis techniques described below, we estimate from this step that ramp-compressed diamond reached a peak pressure of 1400 GPa. The nonisentropic heating contribution from material strength is discussed below.

The Lagrangian analysis method developed by Aidun and Gupta [19] and modified by Rothman *et al.* [20,21] was used to determine the Lagrangian sound speed $C_L(u)$ and $P_x - \rho$ from $u_{fs}(t)$, where u is the particle speed [22]. In all, four shots gave $C_L(u)$ (Fig. 3) and $P_x - \rho$ (Fig. 4) data. $C_L(u)$ and its uncertainty $\sigma_{C_L}(u)$ are obtained from thickness and velocity vs time data by linear regression using errors determined by our measurement accuracies: u_{fs} (0.05 km/s), time (10 ps), and step height (100 nm). The uncertainty is propagated by calculating the weighted mean $\langle C_L \rangle = \sum_j \frac{C_{L,j}}{\sigma_{C_L,j}^2} / \sum_j \frac{1}{\sigma_{C_L,j}^2}$ as shown by the black curve in Fig. 3. The uncertainty in the average value is chosen from the maximum of the uncertainty in the mean and the weighted standard deviation. The resultant sound speeds are consistent with ambient-pressure elastic constants as shown by the (111) longitudinal sound speed (yellow circle) in Fig. 3 [23]. For $u > 2$ km/s the weighted mean can be linearly extrapolated to a value close to the bulk sound speed (blue circle) [24]. $\langle C_L \rangle$ and $\sigma_{\langle C_L \rangle}$ are integrated to obtain $P_x = \rho_0 \int_0^u \langle C_L \rangle du$, $\rho = \rho_0(1 -$

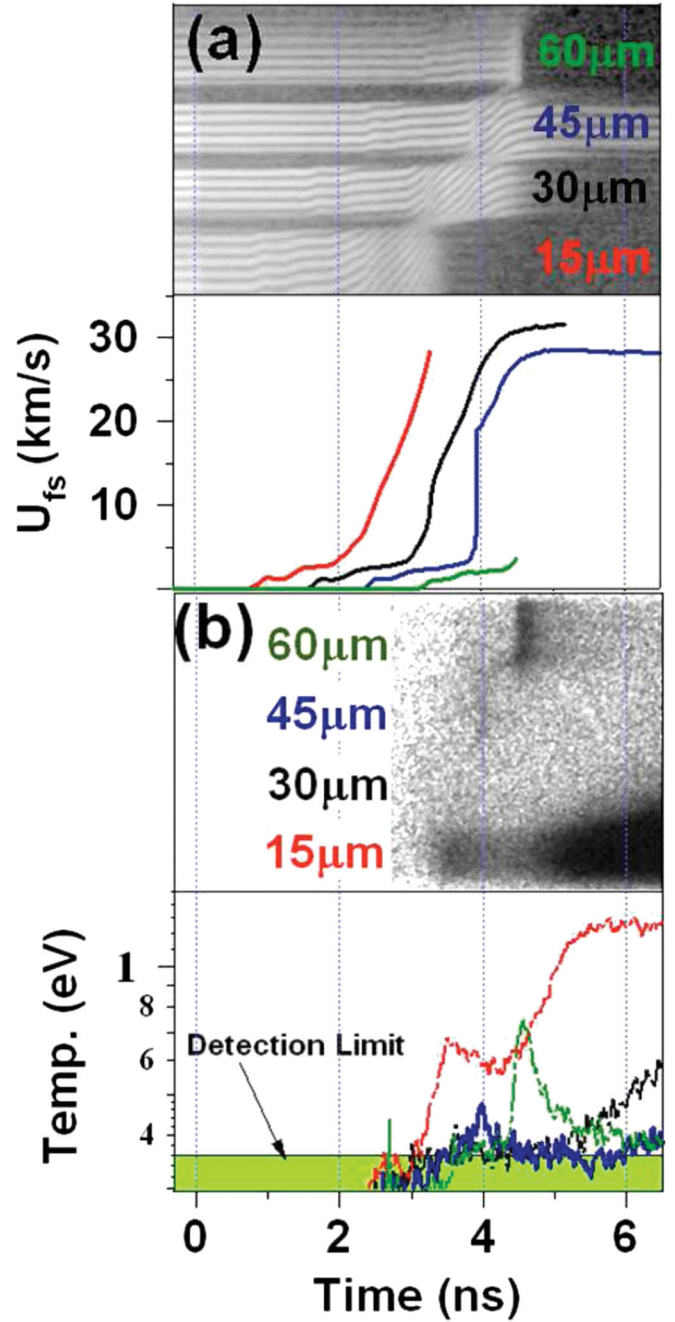


FIG. 2 (color). (a) VISAR data record and analyzed velocity data for ramp-compressed diamond steps. (b) Pyrometer data with lineouts showing inferred temperatures. Different colors indicate data from different step thicknesses sketched in Fig. 1.

$\int_0^u \frac{du}{\langle C_L \rangle})^{-1}$, and their uncertainties $\sigma_{P_x} = \rho_0 \int_0^u \sigma_{\langle C_L \rangle} du$ and $\sigma_\rho = \frac{\rho^2}{\rho_0} \int_0^u \frac{\sigma_{\langle C_L \rangle} du}{\langle C_L \rangle^2}$. Uncertainties are propagated through the integrals linearly, rather than in quadrature, because $\sigma_{\langle C_L \rangle}$ appears to be strongly correlated rather than random. This method of uncertainty propagation allows the direct propagation of experimental uncertainties to $P_x - \rho$.

Figure 3 shows that the Lagrangian sound speed decreases dramatically for $1.1 < u(\text{km/s}) < 1.6$ correspond-

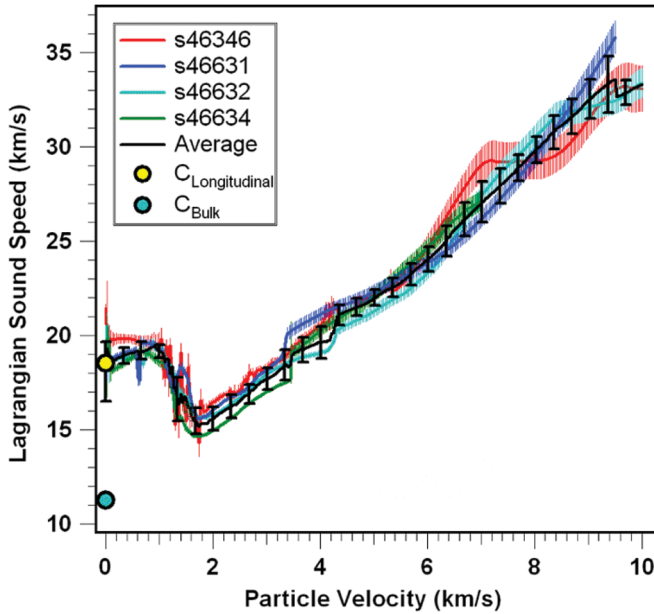


FIG. 3 (color). Lagrangian sound speeds versus particle velocity for 4 different experiments. The black curve is the weighted mean, and yellow and blue circles are the ambient-pressure longitudinal and bulk sound speeds, respectively [23,24].

ing to $74 < P_{x,\text{limit}}(\text{GPa}) < 104$. This is interpreted as the diamond elastic limit, so the initial yield strength of diamond $Y_0 = P_{x,\text{limit}} \frac{1-2\nu}{1-\nu}$ [25], using the Poisson ratio $\nu = 0.07$ [26], gives $69 \leq Y_0(\text{GPa}) \leq 96$. This Y_0 is comparable to shock wave data but is significantly lower than that found in static experiments where $Y_0 = 130\text{--}140$ GPa [26].

The $P_x - \rho$ data for ramp-compressed diamond are shown in Fig. 4. Neither the wave profile $C_L(u)$ or $P_x - \rho$ data show any signature of a phase transition [27] suggesting that diamond is the stable phase up to 800 GPa. Also plotted in Fig. 4 are Hugoniot data from Kondo and Ahrens [28] and Pavlovskii [29] from the solid at $100 < P(\text{GPa}) < 600$ and Brygoo [30], Nagao [31], and Hicks [32] mostly from the melt coexistence phase at $600 < P(\text{GPa}) < 1100$. The Pavlovskii data are plotted along with a correction for the possible existence of a two-wave structure (not observed by Pavlovskii) with a Hugoniot elastic limit of 95 GPa as estimated from Refs. [28,33,34]. The diamond Hugoniot is expected to be close to 9000 K from 600 to 800 GPa and has roughly the same compressibility as the ramp-wave data reported here, in which the temperature is lower. Brygoo *et al.* and Hicks *et al.* report a shift in the Hugoniot ρ upon melting. That there is no shift in the ρ data presented here is because ramp-compressed diamond stays in the diamond phase to at least 800 GPa. Also plotted in Fig. 4 are quasihydrostatic DAC data up to 150 GPa [24], corrected for recent modifications to the ruby pressure calibration [3]. The solid line extending past the DAC data shows an estimated hydrostat

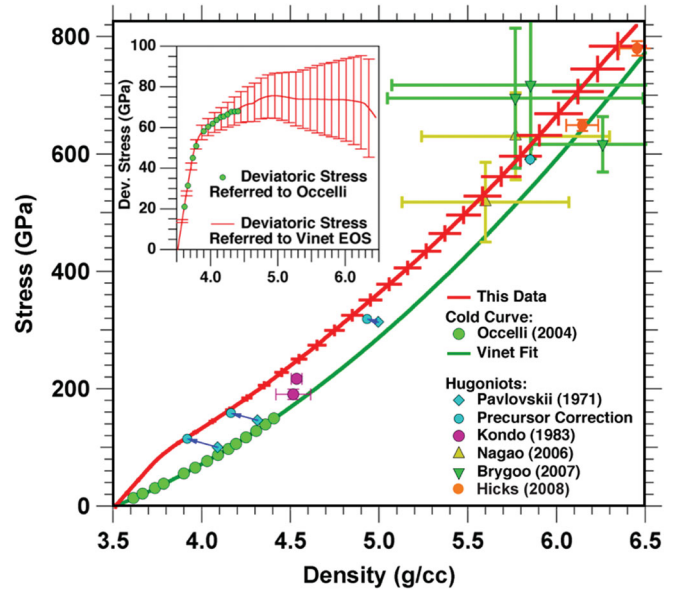


FIG. 4 (color). The main plot shows stress versus density for the weighted mean data in Fig. 3 (red line) compared with measured Hugoniot [28–32] and cold curve [24] data adjusted for the new ruby pressure scale [3]. The blue diamonds represent the original single-wave analysis, and the blue circles show the two-wave corrected analysis of Pavlovskii’s data as discussed in the text. The inset shows the deviatoric stress determined by comparing ramp compression data to the cold curve data (green circles) and a Vinet fit to the data (red line).

up to near 800 GPa based on a Vinet equation of state (EOS) ($\rho_0 = 3.151$ g/cc, $K_0 = 438$ GPa, $K'_0 = 3.68$) fitted to these static data. It is important to note that both the Hugoniot and static data in Fig. 4 used standards, while the RWC $P_x - \rho$ data are absolute, relying only on measured observables.

The inset in Fig. 4 shows the difference in stress between the RWC data and both static data and Vinet fit [35]. While the Vinet extrapolation is certainly a rough guide to the hydrostat at these high P , it provides some context to compare the new solid diamond data reported on here. Assuming that the sample remains on the yield surface $P_x = P + \frac{2}{3}Y$, Fig. 4 gives a rough estimate of the strength above the elastic yield limit and suggests that, after the initial yielding, the yield strength increases slightly and then holds nearly steady up to the highest densities studied. While brittle materials often show a catastrophic loss of strength when shock compressed past the elastic yield point, ramp-compressed diamond appears to retain some strength up to 800 GPa.

From this strength estimate, the T increase due to isentropic compression combined with heating from irreversible processes can be estimated. One such irreversible process is plastic flow. The T rise due to plastic work is $\Delta T_{\text{plastic}} = \int_0^{\Delta W_{\text{plastic}}} \frac{dU}{C(P_f, T)}$, where C is the T -dependent specific heat evaluated at the final pressure P_f , U is the

internal energy per unit mass, and $\Delta W_{\text{plastic}}$ is the plastic work: $\Delta W_{\text{plastic}} = \int \sigma'_{ij} V_0 d\varepsilon^p_{ij} = V_0 \int Y(\eta) \frac{d\varepsilon^p}{d\eta} d\eta$. Here σ'_{ij} is the deviatoric Cauchy stress, $Y(\eta)$ is the flow stress, $d\varepsilon^p_{ij}$ is the plastic-strain increment, $d\varepsilon^p$ is the equivalent plastic-strain increment, and η is the volumetric compression. Since the Debye T of diamond is high (~ 1850 K), C is not in the Dulong-Petit limit and depends on both T and P [36]. The T dependence is estimated by the 3-frequency Einstein model proposed by Reeber and Wang [37], and Wallace [38] provides the $P - \rho$ dependence. In order to compute the plastic-strain increment, the shear modulus from Orlikowski *et al.* is used to convert elastic shear stress to elastic shear strain [39]. From this, the T rise at 600 and 800 GPa is estimated to be ~ 5100 K and ~ 6300 K along the ramp compression path as compared to ~ 9000 and 9000 K on the Hugoniot [6–8]. Note that the reason for the constant T along the Hugoniot is because it intersects the melt curve, while the ramp-compressed diamond remains solid at those pressures.

In summary, diamond was ramp-compressed to a peak pressure of 1400 GPa, and the stress-density relation along this ramp compression path for solid diamond was determined to 800 GPa. Data reveal that the diamond phase of carbon is stable and remains strong under ramped compression to at least 800 GPa. Data presented here are the highest-pressure solid-state data ever collected, and the techniques extend the boundaries of solid-state physics into the TPa regime. Applying these techniques with an optimized 30 ns pulse shape offered by the higher energy National Ignition Facility laser system [40] will potentially ramp-compress a broad range of solids to several TPa.

We acknowledge the outstanding work of C. Wild and E. Woerner of the Fraunhofer Institute for Applied Solid-State Physics, Freiburg, Germany. This work performed under the auspices of the U.S. Department of Energy by Lawrence Livermore National Laboratory under Contract No. DE-AC52-07NA27344.

-
- [1] W.B. Hubbard, *Science* **214**, 145 (1981); J.J. Lissauer, *Nature (London)* **419**, 355 (2002); T. Guillot, *Science* **286**, 72 (1999).
 - [2] L.S. Dubrovinsky *et al.*, *Phys. Rev. Lett.* **84**, 1720 (2000).
 - [3] A. Dewaele, P. Loubeyre, and M. Mezouar, *Phys. Rev. B* **70**, 094112 (2004).
 - [4] P. Reichart *et al.*, *Science* **306**, 1537 (2004).
 - [5] J.H. Eggert *et al.* (to be published).
 - [6] D.K. Bradley *et al.*, *Phys. Rev. Lett.* **93**, 195506 (2004).
 - [7] A.A. Correa, S.A. Bonev, and G. Galli, *Proc. Natl. Acad. Sci. U.S.A.* **103**, 1204 (2006); M.P. Grumbach and R.M. Martin, *Phys. Rev. B* **54**, 15 730 (1996); X.-f. Wang,

- S. Scandolo, and R. Car, *Phys. Rev. Lett.* **95**, 185701 (2005).
- [8] R.L. Kauffman *et al.*, *Phys. Rev. Lett.* **73**, 2320 (1994).
- [9] J. Eggert *et al.*, in *Shock Compression of Condensed Matter*, edited by J.W. Forbes (AIP, Melville, NY, 2007), p. 91.
- [10] R.F. Smith *et al.*, *Phys. Rev. Lett.* **98**, 065701 (2007).
- [11] J.-P. Davis, *J. Appl. Phys.* **99**, 103512 (2006).
- [12] T.R. Boehly *et al.*, *Opt. Commun.* **133**, 495 (1997).
- [13] K.M. Campbell, F.A. Weber, and E.L. Dewald, *Rev. Sci. Instrum.* **75**, 3768 (2004).
- [14] P.M. Celliers *et al.*, *Rev. Sci. Instrum.* **75**, 4916 (2004).
- [15] J.E. Miller *et al.*, *Rev. Sci. Instrum.* **78**, 034903 (2007).
- [16] G.W. Collins *et al.*, *Phys. Rev. Lett.* **87**, 165504 (2001).
- [17] D.G. Hicks *et al.*, *Phys. Rev. Lett.* **97**, 025502 (2006).
- [18] This assumes the emission is coming from the free surface. We estimate the uncertainty in temperature to be 50%.
- [19] J.B. Aidun and Y.M. Gupta, *J. Appl. Phys.* **69**, 6998 (1991).
- [20] S.D. Rothman *et al.*, *J. Phys. D* **38**, 733 (2005).
- [21] S.D. Rothman and J. Maw, *J. Phys. IV* **134**, 745 (2006).
- [22] Only data not affected by either release waves or strong shocks were used to determine $Px - \rho$.
- [23] M.H. Grimsditch and A.K. Ramdas, *Phys. Rev. B* **11**, 3139 (1975).
- [24] F. Occelli, P. Loubeyre, and R. Letoullec, *Nature Mater.* **2**, 151 (2003).
- [25] G.E. Duvall, in *Dynamic Response of Materials to Intense Impulsive Loading*, edited by P.C. Chou and A.K. Hopkins (Air Force Materials Laboratory, Wright Patterson AFB, Dayton, OH, 1972), p. 89.
- [26] M.I. Eremets, I.A. Trojan, P. Gwaze, J. Huth, R. Boehler, and V.D. Blank, *Appl. Phys. Lett.* **87**, 141902 (2005).
- [27] R.F. Smith *et al.*, *Phys. Rev. Lett.* **101**, 065701 (2008).
- [28] K. Kondo and T.J. Ahrens, *Geophys. Res. Lett.* **10**, 281 (1983).
- [29] M.N. Pavlovskii, *Sov. Phys. Solid State* **13**, 741 (1971).
- [30] S. Brygoo *et al.*, *Nature Mater.* **6**, 274 (2007).
- [31] H. Nagao *et al.*, *Phys. Plasmas* **13**, 052705 (2006).
- [32] D.G. Hicks *et al.*, *Phys. Rev. B* **78**, 174102 (2008).
- [33] M.D. Knudson *et al.*, Sandia Report No. SAND2001-3838, 2001.
- [34] R.S. McWilliams *et al.* (to be published).
- [35] P. Vinet *et al.*, *J. Geophys. Res.* **92**, 9319 (1987).
- [36] D.G. Onn, A. Witek, Y.Z. Qiu, T.R. Anthony, and W.F. Banholzer, *Phys. Rev. Lett.* **68**, 2806 (1992).
- [37] R.R. Reeber and K. Wang, *J. Electron. Mater.* **25**, 63 (1996).
- [38] D.C. Wallace, *Thermodynamics of Crystals* (Dover, New York, 1972).
- [39] D. Orlikowski *et al.*, in *Shock Compression of Condensed Matter*, edited by (AIP, Melville, NY, 2007).
- [40] G.H. Miller, E.I. Moses, and C.R. Wuest, *Opt. Eng. (Bellingham, Wash.)* **43**, 2841 (2004).